The kinetics of zinc(II) incorporation into fifty-five free base porphyrins in DMF: structure–reactivity correlations

L. R. Robinson and **P. Hambright***
Department of Chemistry, Howard University, Washington, DC 20059 (U.S.A.)

(Received December 21, 1990)

Abstract

The kinetics of zinc(II) incorporation into fifty-five free base porphyrins of varying charges and structures were investigated in dimethylformamide at 25 °C. The rate law is the same as found by Tanaka and co-workers (*Bull. Chem. Soc. Jpn., 57* (1984) 204) for tetraphenylporphyrin. One interpretation is that Zn(II) forms a complex with the free base porphyrin H_2–P and in a k_1 pathway, the coordinated Zn(II) enters the porphyrin, while in a k_2 route, a second zinc is needed to produce the final product. While little correlation is found between the rate constants and overall porphyrin peripheral charge, k_2 varies over a 26 000 fold range for uncharged species. The replacement of hydrogens by two bulky substituents in the *ortho*-phenyl positions of tetraphenyl type porphyrins leads to a 200–500 fold decrease in k_2, and such *ortho* groups might inhibit porphyrin ring deformation. Phenyl rings substituted in the *para* position by groups such as $-NH_2$,$-OCH_3$ and –OH produce more reactive porphyrins that if such substituents are present in the *meso*-phenyl positions, indicating electron donation to the porphyrin ring by resonance effects. This implies coplanarity between at least one phenyl ring and the porphyrin plane in a distorted metal–porphyrin activated complex. Mercury(II) markedly catalyzes the Zn(II)/H_2–P reactions through the very rapid formation of Hg(II)P, which is 10^4 times more reactive with Zn(II) than H_2–P itself. The predeformed octabromo-tetramesitylporphyrin metallates $\sim 4 \times 10^3$ times faster than the tetramesitylporphyrin.

Introduction

In 1970, Adler and co-workers [1] showed that dimethylformamide (DMF) was a particularly good solvent for the incorporation of many metal ions into porphyrin molecules. Several kinetic studies of such reactions in DMF have appeared, with no general agreement on the mechanism(s) followed [2–5]. We have investigated the rate laws for Zn(II)–porphyrin formation of fifty-five neutral, positive and negatively charged free base (H_2–P) porphyrins as well as seven Zn(II)/Cd(II)–P electrophilic exchange reactions in DMF. Since the Zn(II)/H_2–P process is found to be catalyzed by Hg(II), we also report results for the Hg(II)/H_2–TPP (TPP is tetraphenylporphyrin) reaction which aids in the elucidation of the catalytic behavior. Such work gives an indication of how charge, structure and basicity affect the metallation process.

*Author to whom correspondence should be addressed.

Experimental

The free base porphyrins were samples from previous studies [6–8]. The reaction medium was distilled DMF which was 2.0 M in water, and an ionic strength of 0.72 was maintained by keeping the sum of the molarities of $Ca(NO_3)_2$ and $Zn(NO_3)_2$ (99.999%, Aldrich) equal to 0.24 M. Zinc(II) was analyzed with EDTA and mercury(II) by chloride titrations. The kinetics were run at 25.0 °C on a Beckman DU-70 recording spectrophotometer or a Durrum-Gibson stopped-flow system, with at least a fifty fold excess of metal to porphyrin. Isosbestic points were found throughout the range 700–380 nm, indicating that H_2–P and Zn(II)–P were the major absorbing species. The kinetics were always first order in porphyrin concentration over three half-lives (for reactions that could be followed to completion), with a pseudo-first order rate constant, k_{obs}. For the Zn(II)/H_2–P reactions, at least five different metal ion concentrations, usually over a thirty-two fold range (1.6×10^{-2} to $\sim 5.0 \times 10^{-3}$ M), were investigated for each porphyrin, and for seven prophyrins, lower zinc levels down to $\sim 10^{-4}$ M were employed.

0020-1693/91/$3.50

Results

Zn(II)/H_2–P

Figure 1 shows the kinetic behavior found in the reactions of Zn(II) with tetra(4-aminophenyl)porphyrin [T(4-NH_2)PP]. One mechanism consistent with this pattern is

$$Zn(II) + H_2\text{–}P = (Zn(II)\text{---}H_2\text{–}P) \quad K \tag{1}$$

$$(Zn(II)\text{---}H_2\text{–}P) \longrightarrow \text{products} \quad k_1 \tag{2}$$

$$(Zn(II)\text{---}H_2\text{–}P) + Zn(II) \longrightarrow \text{products} \quad k_2 \tag{3}$$

The free-base porphyrin H_2–P rapidly forms a complex with Zn(II) having an equilibrium constant K. The Zn(II) in this complex is the one that forms the Zn(II)–P in the k_1 pathway, while a second Zn(II) is required to react with this species in the k_2 route. The derived rate law is thus

$$k_{obs} = \{k_1K[Zn(II)] + k_2K[Zn(II)]^2\}/(1 + K[Zn(II)]) \tag{4}$$

Values of K, k_1 and k_2 were determined by a non-linear least-squares program, and Fig. 1 shows the excellent fit of the calculated and observed data for the T(4-NH_2)PP reaction. At high Zn(II) such that $K[Zn(II)] \gg 1$, eqn.(4) reduces to the simpler form

$$k_{obs} = k_1 + k_2[Zn(II)] \tag{5}$$

Above 5.0×10^{-3} M Zn(II), all of the porphyrins followed the rate law in eqn. (5), and k_1 and k_2 are listed in Table 1. For the seven porphyrins studied in detail at low Zn(II) levels, the values of K are shown in Table 2.

Zn(II)/Cd(II)–P

In the exchange reactions of Zn(II) with preformed Cd(II)–porphyrins, the kinetics are first order in Zn(II) and Cd(II)–P concentrations. The rate constants, k_3 for the seven different porphyrins studied are given in Table 3.

Hg(II)/H_2–TPP

Many of the Zn(II)/H_2–P reactions were not complete after standing for many days at 25 °C, and addition of a small crystal of hydrated $Hg(NO_3)_2$ to the reaction mixture rapidly led to the formation of the final Zn(II)–P product. We thus investigated the kinetics of the reaction of tetraphenylporphyrin (H_2–TPP) with Hg(II) in DMF. Making $\sim 5 \times 10^{-6}$ M solutions of H_2–TPP $\sim 10^{-3}$ M in $Hg(NO_3)_2$ produces Hg(II)–TPP, which has its Soret peak at 430.5 nm ($\epsilon = 3.7 \times 10^5$ M^{-1} cm^{-1}). Hg(II)–TPP is easily distinguished from the dinuclear Hg_2–TPP [9, 10], which absorbs at 442 nm, and forms appreciably only above $\sim 10^{-2}$ M Hg(II) levels. The rate law was first order in porphyrin concentration, and one mechanism that explains the Hg(II) dependence is

$$Hg(II) + H_2\text{–}P = \{Hg(II)\text{---}H_2\text{–}P\} \quad k_4, k_{-4} \tag{6}$$

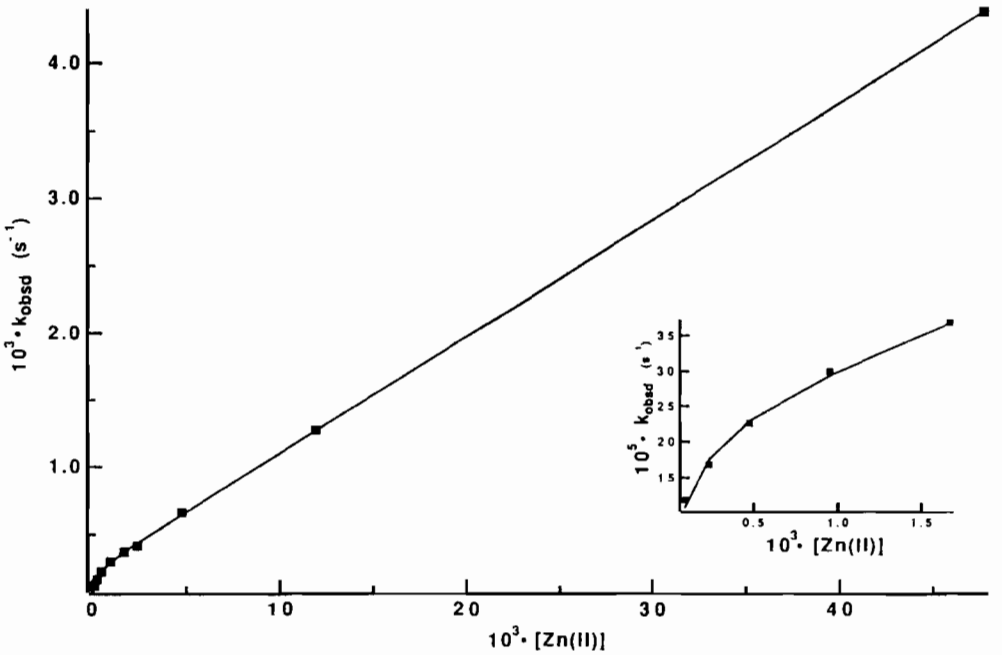

Fig. 1. Plot of k_{obs} vs. Zn(II) for the Zn(II)/H_2–T(4-NH_2)PP reaction in DMF. The squares are the observed data, and the solid line is calculated from eqn. (4), with the parameters from Tables 1 and 2.

TABLE 1. Zinc(II)–porphyrin formation rate constants in DMF, 25 °C.

Porphyrin[a]	Charge	k_1 (s^{-1})	k_2 ($M^{-1}\ s^{-1}$)
H_2–TMPyP(4)	+4	$(9.6\pm1.3)\times10^{-4}$	$(1.5\pm0.1)\times10^{-2}$
H_2–TMPyP(3)	+4	$(3.1\pm0.3)\times10^{-4}$	$(3.6\pm0.4)\times10^{-3}$
H_2–TMPyP(2)	+4	$(6.1\pm1.6)\times10^{-4}$	$(1.2\pm0.2)\times10^{-2}$
t-Ph_2(4-MePy)$_2$	+2	$(7.8\pm1.4)\times10^{-5}$	$(2.2\pm0.2)\times10^{-3}$
t-Ph_2(3-MePy)$_2$	+2	$(3.8\pm1.6)\times10^{-5}$	$(9.7\pm2.1)\times10^{-4}$
t-Ph_2(2-MePy)$_2$	+2	$(3.4\pm0.6)\times10^{-5}$	$(6.3\pm0.7)\times10^{-3}$
T(4-NH_2)PP	0	$(2.5\pm0.1)\times10^{-4}$	$(8.7\pm0.1)\times10^{-2}$
T(3-NH_2)PP	0	$(2.9\pm1.8)\times10^{-5}$	$(2.8\pm0.2)\times10^{-3}$
T(2-NH_2)PP	0		
[4,0]	0	$(5.4\pm0.9)\times10^{-5}$	$(1.8\pm0.1)\times10^{-2}$
[3,1]	0	$(1.6\pm1.3)\times10^{-5}$	$(1.3\pm0.1)\times10^{-2}$
cis [2,2]	0	$(4.7\pm0.2)\times10^{-5}$	$(1.1\pm0.1)\times10^{-2}$
trans [2,2]	0	$(6.1\pm1.1)\times10^{-5}$	$(8.1\pm0.2)\times10^{-3}$
T(4-OH)PP	0	$(4.1\pm0.1)\times10^{-5}$	$(9.9\pm0.4)\times10^{-3}$
T(3-OH)PP	0	$(2.6\pm1.6)\times10^{-5}$	$(1.9\pm0.2)\times10^{-3}$
T(2-OH)PP	0	$(6.8\pm5.9)\times10^{-6}$	$(6.3\pm0.8)\times10^{-4}$
T(4-OCH_3)PP	0	$(2.3\pm1.4)\times10^{-5}$	$(5.1\pm0.4)\times10^{-3}$
T(3-OCH_3)PP	0	$(1.5\pm2.7)\times10^{-5}$	$(2.1\pm0.3)\times10^{-3}$
T(2-OCH_3)PP	0	$(3.5\pm1.2)\times10^{-6}$	$(1.9\pm0.2)\times10^{-4}$
T(2,6-OCH_3)PP	0	$(1.4\pm1.3)\times10^{-7}$	$(1.6\pm0.1)\times10^{-5}$
T(4-CH_3)PP	0	$(3.8\pm0.2)\times10^{-5}$	$(1.1\pm0.1)\times10^{-3}$
T(2-CH_3)PP	0	$(3.7\pm0.3)\times10^{-6}$	$(2.9\pm0.1)\times10^{-4}$
T(2,4,6-CH_3)PP	0	$(4.2\pm0.7)\times10^{-7}$	$(2.4\pm0.1)\times10^{-5}$
H_2–TPP	0	$(1.6\pm0.1)\times10^{-5}$	$(9.7\pm0.2)\times10^{-4}$
H_2–TPP[b]	0	$(3.5\pm0.7)\times10^{-5}$	$(8.6\pm0.2)\times10^{-4}$
T(4-F)PP	0	$(9.3\pm4.6)\times10^{-6}$	$(1.0\pm0.1)\times10^{-3}$
T(2-F)PP	0	$(5.1\pm0.4)\times10^{-6}$	$(9.7\pm0.6)\times10^{-5}$
T(3,5-F)PP	0	$(2.6\pm0.1)\times10^{-5}$	$(5.9\pm0.1)\times10^{-4}$
T(2,6-F)PP	0	$(2.2\pm0.1)\times10^{-6}$	$(3.0\pm0.2)\times10^{-5}$
T(F_5)PP	0	$(2.8\pm0.3)\times10^{-5}$	$(4.5\pm0.8)\times10^{-4}$
T(4-Cl)PP	0	$(4.3\pm1.7)\times10^{-5}$	$(1.5\pm0.2)\times10^{-3}$
T(2-Cl)PP	0	$(1.1\pm0.7)\times10^{-6}$	$(8.3\pm0.8)\times10^{-5}$
T(3,5-Cl)P	0	$(6.8\pm0.3)\times10^{-5}$	$(5.5\pm0.4)\times10^{-4}$
T(2,6-Cl)PP	0	$(2.2\pm0.9)\times10^{-7}$	$(3.0\pm0.9)\times10^{-6}$
T(4-Br)PP	0	$(1.8\pm0.1)\times10^{-5}$	$(6.2\pm0.1)\times10^{-4}$
T(2-Br)PP	0	$(8.2\pm0.4)\times10^{-7}$	$(5.9\pm0.2)\times10^{-5}$
(4-CF_3)PP	0	$(4.4\pm1.3)\times10^{-5}$	$(1.2\pm0.2)\times10^{-3}$
(3-CF_3)PP	0	$(7.2\pm2.3)\times10^{-5}$	$(2.1\pm0.3)\times10^{-3}$
T(4-CO_2CH_3)PP	0	$(2.6\pm0.4)\times10^{-5}$	$(6.6\pm1.1)\times10^{-4}$
T(4-CN)PP	0	$(1.3\pm0.1)\times10^{-5}$	$(7.6\pm0.2)\times10^{-5}$
T(4-NO_2)PP	0	$(2.6\pm0.1)\times10^{-5}$	$(1.1\pm0.1)\times10^{-3}$
T(2-NO_2)PP	0	$(1.9\pm0.2)\times10^{-6}$	$(9.9\pm0.8)\times10^{-5}$
H_2–PF	0	$(4.1\pm1.4)\times10^{-6}$	$(1.1\pm0.2)\times10^{-4}$
C_2–CAP	0	$(3.1\pm1.6)\times10^{-7}$	$(4.5\pm02.)\times10^{-5}$
H_2–OEP	0	$(3.2\pm2.9)\times10^{-6}$	$(7.1\pm0.1)\times10^{-3}$
H_2–ETIO-I	0	$(2.0\pm6.0)\times10^{-6}$	$(4.9\pm0.2)\times10^{-3}$
MP–DME	0	$(1.4\pm0.8)\times10^{-5}$	$(6.8\pm0.2)\times10^{-3}$
DP–DME	0	$(1.9\pm1.8)\times10^{-6}$	$(2.9\pm0.1)\times10^{-3}$
PP–DME	0	$(7.1\pm5.6)\times10^{-6}$	$(2.1\pm0.3)\times10^{-3}$
COPRO-III–TME	0	$(5.5\pm0.2)\times10^{-6}$	$(1.7\pm0.2)\times10^{-3}$
PORPHIN	0	$(1.2\pm0.1)\times10^{-6}$	$(4.1\pm0.2)\times10^{-4}$
(2,4-Br)P–DME	0	$(3.0\pm0.1)\times10^{-5}$	$(3.2\pm0.2)\times10^{-4}$
(2,4-H,CN)P–DME	0	$(4.1\pm0.8)\times10^{-6}$	$(1.5\pm0.1)\times10^{-4}$
H_2–$TPPS_2$	−2	$(1.0\pm0.1)\times10^{-5}$	$(1.1\pm0.1)\times10^{-3}$
H_2–$TPPS_4$	−4	$(1.6\pm0.2)\times10^{-5}$	$(1.8\pm0.1)\times10^{-3}$

[a]H_2–TMPyP(x) are the 4, 3 and 2 isomers of the tetra(*N*-methyl-X-pyridyl)porphyrins, t-Ph_2(X-MePy)$_2$ are the *trans*-diphenyl-di(*N*-methyl-X-pyridyl)porphyrins, T(X-OH)PP is for example tetra(X-hydroxyphenyl)porphyrine, H_2–TPP is tetraphenylporphyrin, H_2–PF is the [4,0]-picket fence porphyrin, C_2-CAP is the C_2-capped porphyrin, H_2–OEP is octaethylporphyrin, H_2–ETIO-I is etioporphyrin-I, MP–, DP– and PP–DME are the dimethylesters of *meso*, deutero and protoporphyrin-IX, COPRO-III–TME is the tetramethylester of coproporphyrin-III, H_2–$TPPS_2$ is *trans*-diphenyl-di(4-sulfonatophenyl)porphyrin, and H_2–$TPPS_4$ is tetra(4-sulfonatophenyl)porphyrin. [b]Data from Ref. 4.

TABLE 2. Zinc(II)/H_2–P equilibrium constants in DMF, 25 °C

Porphyrin	K (M^{-1})
H_2–TPP[a]	$(7.2\pm1.5)\times10^2$
H_2–TPP	$(12.3\pm3.4)\times10^3$
T(2,6-F)PP	$(2.8\pm0.5)\times10^3$
T(4-NH_2)PP	$(7.7\pm1.2)\times10^3$
T(4-$(CH_3)_2N$)PP	$(6.0\pm3.1)\times10^3$
T(4-OH)PP	$(9.5\pm1.0)\times10^3$
$TPPS_4$	$(2.3\pm0.4)\times10^3$
$TPPS_2$	$(3.0\pm0.4)\times10^3$

[a]Result from Ref. 4.

$$\{Hg(II)\text{---}H_2\text{–}P\} + Hg(II) \longrightarrow Hg(II)\text{–}P + 2H^+ + Hg(II) \quad k_5 \quad (7)$$

With $\{Hg(II)\text{---}H_2\text{–}P\}$ as a steady-state intermediate, the derived rate law is of the form

$$k_{obs} = k_4k_5[Hg(II)]^2/(k_{-4} + k_5[Hg(II)]) \quad (8)$$

Thus, a plot of $\{[Hg(II)]^2/k_{obs}\}$ versus [Hg(II)] should be linear, with an intercept of $[k_{-4}/(k_4k_5)]$ and a slope of $(k_4)^{-1}$. Such a relationship is shown in Fig. 2, with $k_4 = (2.1\pm0.2)\times10^4$ M^{-1} s^{-1} and $[k_{-4}/k_5] = (3.2\pm0.9)\times10^{-4}$ M.

Discussion

In 1972, Meot-Ner and Adler used a single concentration of $CuCl_2$ in DMF at various temperatures to obtain activation free energies for Cu(II)–P formation [2]. Longo *et al.* [3] in 1973 examined in detail the kinetics of incorporation of various transition metals into fifteen free base porphyrins by an initial rate method in DMF, and concluded that the reactions were first order in metal and porphyrin concentration. Tanaka and colleagues [4] studied this reaction at substantially lower metal ion concentrations in DMF, and suggested in 1984 that the metal and H_2–TPP first formed a complex (K), and then either the metal ion dropped directly from this complex into the porphyrin (k_1), or in a second (k_2) pathway, the complex reacted with a second metal ion to produce the final metalloporphyrin. Their values of K were 1.6×10^4 M^{-1} for Cu(II), 7.2×10^2 M^{-1} for Zn(II), and no kinetic evidence for complex formation was found for Cd(II). Our observed Zn(II) incorporation rate behavior for fifty-four of the porphyrins is in agreement with that reported by Tanaka. Within experimental error, our values of k_1 and k_2 for H_2–TPP are the same (Table 1) as found by them earlier, while our K is about seventeen times higher (Table 2). The K values for the seven porphyrins studied at low zinc levels average to $(6\pm3)\times10^3$ M^{-1}, and since they are relatively insensitive to the magnitudes of k_1 and k_2 found, no effort was made to measure K for all of the compounds reported. From the Zn(II) concentrations used, all derivatives in Table 1 have $K > 10^3$ M^{-1}. While we follow Tanaka in postulating that the kinetically determined complex lies along the reaction pathway, it is noted that the same kinetic behavior obtains if this complex were viewed as a dead-end intermediate, and steady-state kinetics alone will not distinguish between these two reaction mechanisms [11].

Pasternack's group [12] investigated the Cu(II)/H_2–TPP reaction in another non-aqueous solvent, DMSO, and kinetically found a K of 5 M^{-1}, with no evidence for k_2. In the examination of Cu(II) incorporation into long chain picket fence porphyrins in 9:1 DMF–H_2O, Barber and Whitten [13] mentioned that their k_{obs}/[Cu(II)] values increased with decreasing Cu(II) levels, and this is the behavior predicted by eqn. (5). If only a limited range of high metal ion concentrations is studied in porphyrin metallation reactions in DMF, it is not difficult to conclude that the process is simply first order in metal and porphyrin concentration, as the observed intercepts of plots of k_{obs} versus [M(II)] are small.

TABLE 3. Kinetic results for the reactions of cadmium–porphyrins with Zn(II)

Porphyrin[a]	Charge	k_3 (M^{-1} s^{-1})	k_3(Zn/Cd–P)/k_2(Zn/(Zn--H_2–P)
Cd–TMPyP(4)	+4	(1.0 ± 0.1)	6.7×10^1
Cd–TMPyP(3)	+4	$(4.2\pm0.1)\times10^{-1}$	1.1×10^2
Cd–TMPyP(2)	+4	(1.3 ± 0.1)	1.1×10^2
Cd–t-Ph_2(4-MePy)$_2$	+2	(4.0 ± 0.1)	1.8×10^4
Cd–t-Ph_2(2-MePy)$_2$	+2	(1.9 ± 0.1)	3.0×10^2
Cd–TPP	0	$(2.8\pm0.1)\times10^1$	1.4×10^4
Cd–t-Ph_2(2-EtPy)$_2$	+2	$(9.1\pm2.0)\times10^{-1}$	

[a]TMPyP(X) is tetra(*N*-methyl-X-pyridyl)porphyrin, t-Ph_2(X-MePy)$_2$ is the *trans*-diphenyl-di(*N*-methyl-X-pyridyl)porphyrin, TPP is tetraphenylporphyrin.

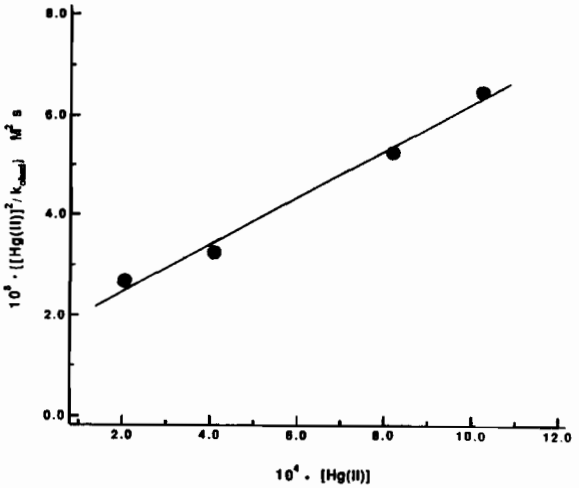

Fig. 2. Plot of $\{Hg(II)^2/k_{obs}\}$ vs. Hg(II) for the Hg(II)/H_2–TPP reaction in DMF.

As Tanaka and co-workers [4] have pointed out, the reported rate constants under these conditions closely approximate the value of k_2 in the detailed mechanism. Thus, Lavallee and Onady [5] showed that in the k_2 pathway, H_2–TPP and D_2–TPP react with $Zn(DMF)_6^{2+}$ at equal rates, implying the lack of a kinetic isotope effect in this k_2 route.

With pre-deformed, higher basicity centrally N-alkylated porphyrins, which react about 10^3 times faster than the parent unmethylated substrates, all reports [4, 14–16] indicate that these reactions in DMF (and water [17]) are simply first order in metal and porphyrin concentration, and the same is usually found with water soluble H_2–P porphyrins in aqueous solution [18–20]. The activated complex in our heterodinuclear Zn/Cd(II)–P exchange reactions has the composition (Zn–P–Cd), and the rapidity of such reactions as compared to uncatalyzed incorporations is usually ascribed in part to the coordinated Cd(II) deforming the planar porphyrin nucleus in such a manner that a second metal ion is more readily able to incorporate into this bent porphyrin structure. As such, the k_2 pathway, with an activated complex of composition (Zn–H_2P–Zn) can be viewed as the homonuclear counterpart of the heterodinuclear reactions, where the bound zinc ion causes deformation, leading to a more rapid loss of protons, facilitating the subsequent incorporation of a second metal ion [4, 18]. In line with crystal structure data [21], the two metal ions in the heterodinuclear activated complex are assumed to lie on opposite sides of the porphyrin plane. However, the C_2-capped and tetra(alpha)-picket fence porphyrins, in which both sides of the porphyrin plane are definitively non-equivalent, show the same Zn(II) incorporation kinetic behavior as the more symmetrical porphyrins, and hence the geometry of such activated complexes is not obvious from these experiments.

Other workers [4, 22] have shown that the reactions of uncharged porphyrins with divalent cations in DMF show rate constants that are independent of ionic strength, and we also find the same observed rate constants at all Zn(II) levels in the absence of added $Ca(NO_3)_2$. Tetrapositive porphyrins are predicted to react with Zn(II) about 10^6 times slower than tetranegative derivatives [23] when extrapolated to zero ionic strength in high dielectric constant aqueous solutions, and the relative rate differences decrease with an increase in ionic strength. However, we find similar rate constants for the tetrapositive TMPyP(4) and tetranegative $TPPS_4$ porphyrins in the low dielectric DMF media, implying that these charged species react as tightly ion-paired derivatives. Thus the rate differences attributed to overall porphyrin charge noted in water [24] are absent in DMF.

Table 1 indicates that for the most part, k_1 and k_2 parallel one another and further discussion will mainly be in terms of the more accurately determined k_2. $E_{1/2}(1)$ is the reduction potential in volts of the free base porphyrin to its radical anion form, and such values are known in DMF for most of the porphyrins studied [6, 8].

$$H_2\text{–}P + e^- = H_2\text{–}P^- \qquad E_{1/2}(1) \tag{9}$$

For the beta-pyrrole substituted compounds, $E_{1/2}(1)$ has been shown to be linearly related to the basicity of the porphyrin, where the basicity is in terms of pK_3 for the dissociation of the mono-cation H_3–P^+ into the free base H_2–P, measured in detergent solutions [8].

$$H_3\text{–}P^+ = H_2\text{–}P + H^+ \qquad K_3 \tag{10}$$

Figure 3 shows the linear relationship between log k_2 and $E_{1/2}(1)$ for these beta-pyrrole porphyrins. The rate constants increase by a factor of six for a ten fold increase in porphyrin basicity.

With phenyl-substituted tetraphenyl type porphyrins, Meot-Ner and Adler estimated pK values for the H_4–P^{2+}/H_2–P reaction by $HClO_4$ titrations in DMF [25]. Figure 4 shows that for these derivatives, there is no linear correlation between pK and $E_{1/2}(1)$. However, a graph of log k_2 versus pK is linear for the porphyrins of known pK, and thus we assigned pKs for the remainder of the *para*-substituted porphyrins based on their known $E_{1/2}(1)$ values, and this log k_2/pK correlation is shown in Fig. 4. The specific rates increase by a factor of 3 for a ten fold increase in basicity.

The H_3–P^+/H_2–P reaction involves a relatively planar free base porphyrin transforming into a non-

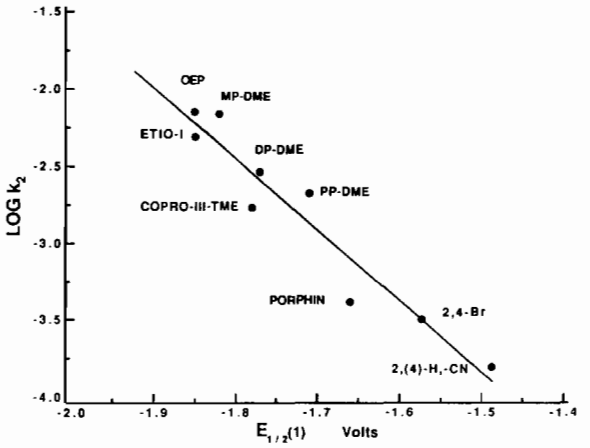

Fig. 3. Plot of log k_2 vs $E_{1/2}(1)$ for Zn(II)/H_2–P reactions of beta-pyrrole substituted porphyrins.

planar mono-cation, and the linearity of the pK_3/$E_{1/2}(1)$/log k_2 plots gives little information on this deformation with beta-pyrrole substituted porphyrins. The curvature in the pK/$E_{1/2}(1)$/log k_2 graphs indicates that porphyrins with phenyl groups bearing the *para*(4) $-NH_2$, $-N(CH_3)_2$, –OH and $-OCH_3$ substituents are donating electron density by resonance to the porphyrin ring, facilitating protonation and metal incorporation for both Zn(II) and Cu(II) [2, 3, 25]. The corresponding groups in the *meta*(3) phenyl positions, in which resonance cannot occur, do not show such excess kinetic reactivity (Table 1). Hammett type analysis on the pK values show a 60% resonance and 40% inductive contribution [25].

If the porphyrin ring deforms, the phenyl ring(s) can rotate coplanar with the porphyrin nucleus, and maximize this resonance interaction. The implication is that the porphyrin in the activated complex in such metal incorporation reactions in non-planar in geometry. With the same phenyl porphyrins, there is a linear relationship [6] between $E_{1/2}(1)$ and $4\sigma_p$, indicating that phenyl ring rotation is not necessary when an electron is added to the free base porphyrin to produce the radical anion. Furthermore, $E_{1/2}(1)$ is similar for porphyrins with the same *ortho*, *meta* and *para* substituent.

When considering uncharged porphyrins, Table 1 shows a twenty-six thousand fold decrease in k_2 in passing from the very reactive tetra(4-aminophenyl)porphyrin to the slower tetra(2,6-dichlorophenyl)porphyrin. Substituents in the *ortho*(2)-phenyl positions make the porphyrin less basic towards protons [25], perhaps by preventing the porphyrin nucleus from readily deforming into a non-planar configuration. Space filling models also indicate that such groups can also sterically block the incoming metal from the central nitrogen atoms. For the chlorophenyl porphyrins, the relative k_2 values are in the order 1:27:500 for the 2,6-dichloro, 2-chloro and 4-chlorophenyl derivatives, respectively, and Fig. 5 shows related trends for a variety of 2,6-, 2- and 4-substituted derivatives. In addition, the 3,5-difluoro and dichlorophenyl porphyrins are about an order of magnitude more reactive than their 2,6- counterparts which have substituents closer to the reaction

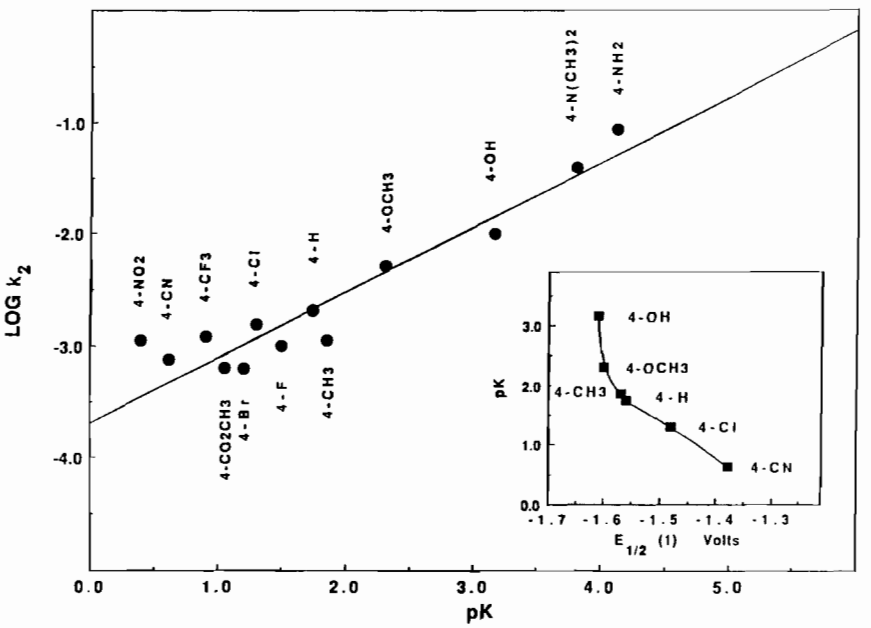

Fig. 4. Insert: the relationship between pK and $E_{1/2}(1)$ for *para*-substituted tetraphenylporphyrins of known basicity. The main figure is a plot of log k_2 vs. pK for a series of *para*-substituted tetraphenylporphyrins.

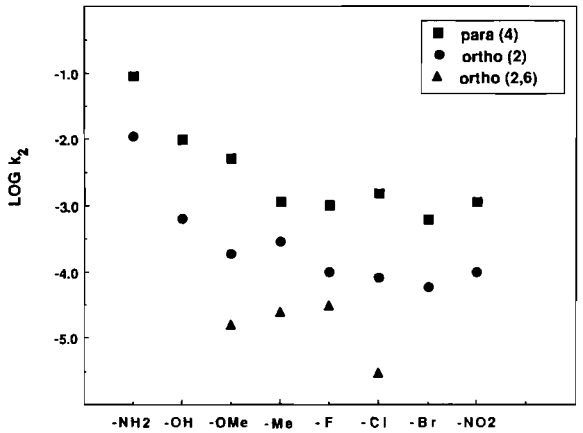

Fig. 5. The variation in log k_2 for the Zn(II)/H_2–P reaction is shown for various *para*, *ortho* and *ortho* di-substituted tetraphenylporphyrins.

center. Bulky *ortho* substituents also increase the activation energy for phenyl ring(s) rotating into planarity with the porphyrin nucleus [26], thus decreasing the resonance contributions that such substituents could make to the incorporation process.

The different atropisomers of T(2-NH_2)PP react at slightly different rates, and this same order has been found with Cu(II) in DMF for a variety of *ortho*-phenyl substituted picket fence type atropisomers of varying sizes [13, 27]. The order (4,0) > (3,1) > *cis*(2,2) > *trans*(2,2) could reflect steric factors, where the metal enters the less hindered face in the (4,0) and (3,1) isomers, and with both-side addition in the *cis* and *trans* (2,2) species. Specific solvations [28] and the differing tendencies of such derivatives to adopt non-planar reactive configurations must also be considered.

The reaction of octabromo-tetra(2,4,6-trimethylphenyl)porphyrin [29] with Zn(II) was briefly studied. Here, $k_1 = (1.6 \pm 0.1) \times 10^{-3}\ s^{-1}$, $K = (49 \pm 6)\ M^{-1}$ and $k_2 = 0$. This porphyrin is 3900 times more reactive than the tetra(2,4,6-trimethylphenyl)porphyrin. Models indicate that the eight bulky bromo groups on the porphyrin beta-pyrrole positions give the free base a slightly non-planar geometry, which could lead to the rapid metallation of this sterically-hindered derivative, and as such is reminiscent of the enhanced reactivity of the centrally N-alkyl porphyrins noted above.

The rate for the Zn(II)/Cd(II)–P reactions are first order in metal and preformed Cd(II)–P, and similar results have been found in pyridine [30, 31] and aqueous media [32, 33]. As shown in Table 3, these exchange reactions are from 60 to 18 000 times faster than k_2 for the corresponding zinc incorporation into the (Zn(II)--H_2–P) form of the porphyrin. The large cadmium ion cannot fit into the porphyrin plane, and may distort the macrocycle such that it is more reactive with an incoming metal that can irreversibly form a metalloporphyrin.

The Zn(II)/H_2–P reactions are found to be catalyzed by addition of small quantities of Hg(II), Qualitatively, porphyrins that reacted fastest with Zn(II) showed the most rapid mercury catalysis. To understand such Hg(II) effects, the reaction between Hg(II) and H_2–TPP was investigated. The interpretation is that {Hg(II)---H_2–P} is formed as a steady-state intermediate, and reacts with another Hg(II) to produce observed Hg(II)–TPP product. Just as with Zn(II), two Hg(II) ions are required to form the final metalloporphyrin in DMF. The relative rates of metals reacting with H_2–TPP (k_2 terms) are Hg(II) ≫ Cu(II) ~ Cd(II) > Zn(II) in the order $10^7 \gg 25 \sim 22 > 1$, and a similar trends was found for metal incorporation into N–Me–TPP in DMF [20]. In comparison to the other metal ions, the large size of Hg(II), its lability and tendency for linear and tetrahedral coordination might indicate that less and more rapid metal ion coordination shell rearrangement occurs for Hg(II), which leads to enhanced porphyrin incorporation rates.

Preliminary data for Zn(II)/Hg(II)–TPP indicates a rate law first order in Zn(II) and Hg(II)–TPP, with a specific rate constant of $\sim 10^2\ M^{-1}\ s^{-1}$. The relative rate constants for the bimolecular reactions of Zn(II) with Hg(II)–TPP, Cd(II)–TPP and H_2–TPP in DMF are in the order $6 \times 10^4 : 1.4 \times 10^4 : 1$, respectively. The Hg(II) catalysis of the Zn(II)/H_2–P systems is then due to the extremely fast reaction of Hg(II) with unreacted H_2–P producing Hg(II)–TPP, and its subsequent rapid reaction with Zn(II) forming the Zn(II)–P product. The addition of Cd(II) to the Zn(II)/H_2–P reaction mixture does not as markedly catalyze product formation, since the reaction of Cd(II) with H_2–P is orders of magnitude slower than that of Hg(II). Such Hg(II) catalysis has been used to measure the equilibrium constant for Zn(II)–$TPPS_4$ formation in water [34], where Hg_2–$TPPS_4$ may be one of the reaction intermediates [9]. The catalysis of such incorporation reactions has been shown [31, 35, 36] to be in the order Hg(II) ≫ Cd(II) > Pb(II), and this parallels both the formation rates of the intermediates, and their reactivity with the final metal ion.

Acknowledgement

We thank the Howard University Faculty Research Support Program for financial support.

References

1 A. Adler, F. Longo, F. Kampas and J. Kim, *J. Inorg. Nucl. Chem., 32* (1970) 2443.
2 M. Meot-Ner and A. Adler, *J. Am. Chem. Soc., 94* (1972) 4763.
3 F. Longo, E. Brown, D. Quimbly, A. Adler and M. Meot-Ner, *Ann. NY. Acad. Sci., 206* (1973) 420.
4 S. Funahashi, Y. Yamaguchi and M. Tanaka, *Bull. Chem. Soc. Jpn., 57* (1984) 204.
5 D. Lavallee and G. Onady, *Inorg. Chem., 20* (1980) 907.
6 P. Worthington, P. Hambright, R. Williams, J. Reid, C. Burnham, A. Shamim, J. Turay, D. Bell, R. Kirkland, R. Little, N. Datta-Gupta and U. Eisner, *J. Inorg. Biochem., 12* (1980) 281.
7 G. Nahor, P. Neta, P. Hambright, A. Thompson and A. Harriman, *J. Phys. Chem., 93* (1989) 6181.
8 P. Worthington, P. Hambright, R. Williams, K. Smith and K. Langry, *Inorg. Nucl. Chem. Lett., 16* (1980) 441.
9 A. Adeyemo and M. Krishnamurthy, *Inorg. Chem., 16* (1977) 335.
10 M. Hudson and K. Smith, *Tetrahedron, 32* (1976) 597.
11 R. Langley and P. Hambright, *Inorg. Chem., 24* (1985) 3716.
12 R. Pasternack, G. Vogel, C. Skowronek, R. Harris and J. Miller, *Inorg. Chem., 20* (1981) 3763.
13 D. Barber and D. Whitten, *J. Am. Chem. Soc., 109* (1987) 6842.
14 B. Shah, B. Shears and P. Hambright, *Inorg. Chem., 10* (1971) 1828.
15 D. Lavallee, *The Chemistry and Biochemistry of N-Substituted Porphyrins,* VCH, New York, 1987.
16 S. Funahashi, Y. Yamaguchi and M. Tanaka, *Inorg. Chem., 23* (1984) 2249.
17 S. Funahashi, Y. Ito, H. Kakito, M. Imano, Y. Hamada and M. Tanaka, *Mikrochim. Acta, 4* (1986) 33.
18 P. Hambright, in K. M. Smith (ed.), *Porphyrins and Metalloporphyrins* Elsevier, Amsterdam, 1977, Ch. 6.
19 D. Lavallee, *Coord, Chem. Rev., 61* (1985) 55.
20 M. Tabata and M. Tanaka, *Inorg. Chem., 27* (1988) 203.
21 M. Tsutsui and G. A. Taylor, in K. M. Smith (ed), *Porphyrins and Metalloporphyrins,* Elsevier, Amsterdam, 1977, Ch. 7.
22 M. Bain-Ackerman and D. Lavallee, *Inorg. Chem., 18* (1979) 3358.
23 J. Nwaeme and P. Hambright, *Inorg. Chem., 23* (1984) 1990.
24 A. Adeyemo, A. Shamim, P. Hambright and R. Williams, *Ind. J. Chem., 21 A* (1982) 763.
25 M. Meot-Ner and A. Adler, *J. Am. Chem. Soc., 97* (1975) 5107.
26 R. Freitag and D. Whitten, *J. Phys. Chem., 87* (1983) 3918.
27 J. Turay and P. Hambright, *Inorg. Chim. Acta, 53* (1981) L147.
28 A. Valiotti, A. Adeyemo, R. Williams, L. Ricks, J. North and P. Hambright, *J. Inorg. Nucl. Chem., 43* (1981) 2653.
29 P. Hoffman, G. Labat, A. Robert and B. Meunier, *Tetrahedron Lett., 31* (1990) 1991.
30 J. Reid and P. Hambright, *Inorg. Chim. Acta, 33* (1979) L135.
31 C. Grant and P. Hambright, *J. Am. Chem. Soc., 91* (1969) 4195.
32 M. Tabata and M. Tanaka, *J. Chem. Soc., Dalton Trans.,* (1983) 1955.
33 A. Shamim and P. Hambright, *Inorg. Chem., 19* (1980) 564.
34 M. Tabata and M. Tanaka, *J. Chem. Soc., Chem. Commun.,* (1985) 42.
35 M. Tanaka, *Pure Appl. Chem., 55* (1983) 151.
36 S. Haye and P. Hambright, *Inorg. Chem., 23* (1984) 4777.